Room Temperature Ferromagnetism in Vacuum-Annealed CoO Nanospheres

Guijin Yang, Daqiang Gao, Zhenhua Shi, Zhaohui Zhang, Jing Zhang, Jinlin Zhang, and Desheng Xue*

Key Laboratory for Magnetism and Magnetic Materials of MOE, Lanzhou University, Lanzhou 730000, P. R. China

Received: July 22, 2010; Revised Manuscript Received: November 11, 2010

Single-crystalline CoO nanospheres with the size distribution between 40 and 250 nm were prepared by a solvothermal method. Magnetic measurements indicate that the vacuum-annealed samples show room temperature ferromagnetism except for the CoO nanospheres of 250 nm, which still exhibit paramagnetism after being postannealed in vacuum atmosphere (10^{-3} Pa) at 250 °C as others. The saturation magnetization of all postannealed samples monotonically increases with the decrease of nanosphere diameter. No other impurity phases are observed for the postannealed samples, indicating that the revealed ferromagnetism is an intrinsic property. The fitted XPS results of O 1s spectra indicate that the variations of oxygen vacancies concentration are consistent with the variations of saturation magnetization for the vacuum-annealed samples, suggesting that the formed oxygen vacancies at the surface of the CoO nanospheres during the vacuum-annealing process account for the observed ferromagnetism.

Introduction

Traditional nonmagnetic oxide materials, such as ZnO, CeO_2, CuO, HfO_2, CoO, and MgO, have attracted great attention due to their unexpected room temperature (RT) ferromagnetism (FM) in recent years.[1−6] However, the origin of the observed RT FM in these nanostructures is still unclear:[7,8] Some experimental and theoretical works indicated that the observed RT FM is attributed to the grain boundaries or cation vacancies,[9−11] while other related studies showed that the nonintrinsic FM is due to the formation of ferromagnetic clusters, bound magnetic polarons, and metal-deficient centers.[12,13] In addition, some investigations have suggested that oxygen vacancies (surface/interface) might be responsible for the observed RT FM of oxide nanostructures.[4,14−16]

CoO nanostructure, typically owning rock-salt phase (dark yellow color) and wurtzite phase (green color),[17] has been considered as an important industrial material for various practical applications, such as catalysis, gas sensors, and lithium-ion batteries.[18−20] Recently, the RT FM of CoO nanocrystals (bulk CoO is antiferromagnetic with $T_N \approx 290$ K) also attracted much attention due to its potential applications in spintronics.[21] The core−shell model was initially developed to interpret the observed RT FM in CoO nanoparticles.[5] Wdowik et al. have demonstrated that cation vacancies can account for the FM properties of CoO nanostructures based on the first-principles calculation.[22] Meanwhile, Dutta et al. also reported the observation of RT FM in pure CoO nanoparticles after annealing the precursor under nitrogen for 6 h. They considered that there was an increase in anionic vacancies with increasing annealing time.[23] Therefore, the origin of RT FM for the CoO nanostructure is still controversial. It is imperative and necessary to devote more efforts to the properties of CoO nanostructure to explore the actual cause of RT FM. In this work, we synthesize different diameter single-crystalline CoO nanospheres with a pure rock-salt phase by solvothermal method and discuss the origin of RT FM in the CoO nanospheres under vacuum-annealing.

Experiment

CoO nanospheres were prepared by the traditional solvothermal method. The purity of all chemicals is analytical, used without any further treatment. In a typical synthesis process, 1.993 g of cobalt acetate powder was dissolved into 50 mL of anhydrous ethanol, and then 0.3 mL of ethanolamine was added into the solution under continuous agitation using a magnetic stirrer. After stirring for 1 h, the solution was then placed into an 80 mL Teflon-lined autoclave to react at 180 °C for 12 h. The resulted suspension was naturally cooled down to RT. The reacted mixture with dark yellow crystals was collected by centrifugation and washed with ethanol several times. The obtained CoO nanoparticles were uniformly dispersed in ethanol and dried in a vacuum oven at RT for 24 h. Four samples were prepared through controlling the cobalt acetate concentration (0.32, 0.16, 0.08, and 0.04 M). For convenience, the four as-prepared samples were labeled by S1, S2, S3, and S4, respectively. Then the four samples were annealed in low vacuum atmosphere (10^{-3} Pa) at 250 °C for 2 h and marked as S1-250, S2-250, S3-250, and S4-250, respectively.

The crystalline structures of the samples were investigated by X-ray diffraction (XRD, X′ Pert PRO PHILIPS, CuKa radiation, $\lambda = 1.540\,56$ Å). The morphology and microstructures of the CoO nanospheres were studied by scanning electron microscopy (SEM, Hitachi S-4800) and high-resolution transmission electron microscopy (HRTEM, JEM-2010). The chemical states of different elements presented in CoO were analyzed by X-ray photoelectron spectroscopy (XPS, VG ESCALAB 210); the standard C 1s peak at 285.0 eV was used as a reference for correcting the shifts. The magnetic properties of CoO nanospheres were measured by a vibrating sample magnetometer (VSM, Lakeshore 7304) and a quantum design magnetic property measurement system (MPMS) based on a superconducting quantum interference device (SQUID).

* To whom correspondence should be addressed. E-mail: xueds@lzu.edu.cn.

10.1021/jp106818p
Published on Web 12/02/2010

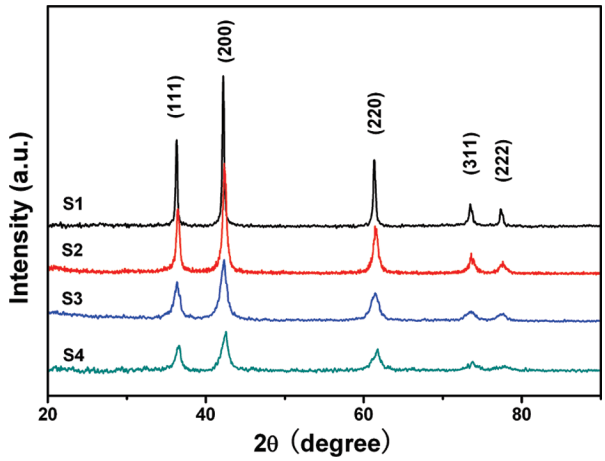

Figure 1. XRD patterns of the as-prepared samples (S1, S2, S3, and S4).

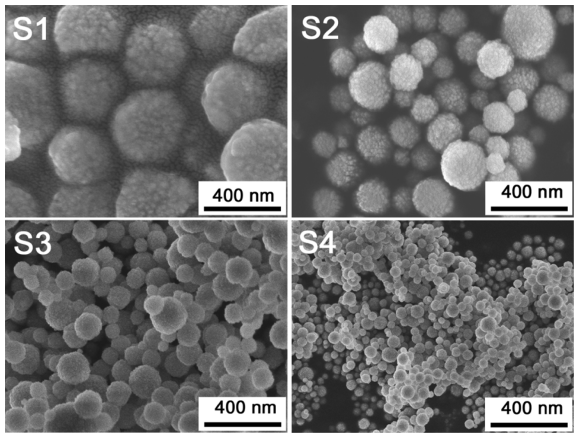

Figure 2. SEM images of the as-prepared samples (S1, S2, S3, and S4).

Results and Discussion

Typical XRD patterns of as-prepared CoO nanoparticles are shown in Figure 1, of which cobalt acetate concentrations are 0.32, 0.16, 0.08, and 0.04 M correspondingly. The peak positions of all four concentration samples are identical, which can be assigned to (111), (200), (220), (311), and (222) lattice planes of CoO structure with rock-salt structure, respectively (JCPDS card no. 431004; space group, $Fm\bar{3}m$). No diffraction peaks of Co_3O_4 or metallic Co are observed. The full width half-maximum (fwhm) of the diffraction peaks increases gradually with the decrease of cobalt acetate concentration. The average crystalline sizes can be estimated to be around 49, 19, 9, and 7 nm for S1, S2, S3, and S4 with the Scherrer formula, respectively.

The morphologies of the as-prepared CoO nanocrystals were analyzed by SEM, and the results are shown in Figure 2. It can be seen that the shapes of all CoO particles are nanospheres which are made up of many CoO spherical nanoparticles. The average diameters of CoO nanospheres are about 250, 150, 100, and 40 nm individually, decreasing with the decrease of cobalt acetate concentration.

The morphology and structure of CoO nanospheres were further investigated by HRTEM. Figure 3a and 3b show two typical low-magnified and large-magnified TEM photographs of sample S2. The feature of small CoO nanoparticles stinging on the surface of individual CoO nanospheres can be seen in both photos. The average of these CoO nanospheres is about

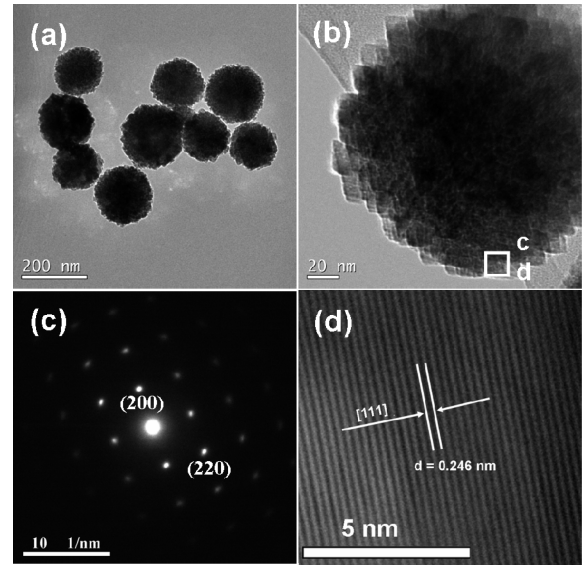

Figure 3. (a) Typical TEM image and (b) TEM image of a single nanosphere; (c) SAED pattern and (d) HRTEM image of sample S2.

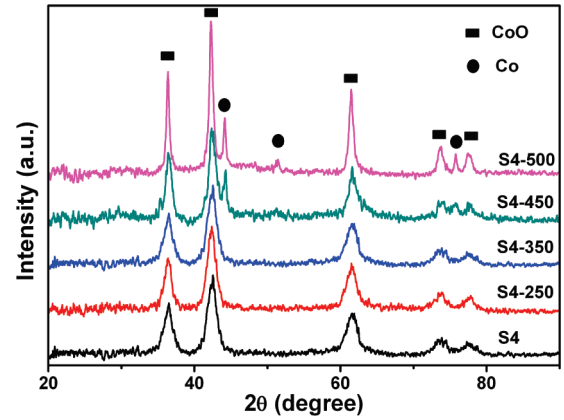

Figure 4. XRD patterns of the sample S4 postannealed under vacuum at different temperatures.

150 nm, consistent with above SEM observation (Figure 2). The SAED pattern of single nanoparticle is shown in Figure 3c, revealing a single crystal with cubic structure. The spots can be indexed as (200), (220), and so on. There are no other diffraction spots or rings of Co or Co_3O_4 observed, indicating the purity phase of the CoO nanocrystals, well consistent with the XRD analysis above. Figure 3d shows a high-resolution lattice imaging also indicating that individual CoO nanospheres are single crystal, of which lattice spacing is 2.46 Å, corresponding to (111) lattice planes.

Magnetic measurements indicate that all the as-prepared CoO nanospheres are paramagnetic (not shown here). Experimental and theoretical studies show that the defects at the surface of nanograins and oxygen vacancies during vacuum annealing can lead to RT FM in nanocrystalline materials.[24,25] However, in our case, the postannealed CoO nanoparticles may be introduced as Co magnetic impurities into the samples. In order to explore the optimum annealing temperature, the sample S4 which possesses the minimum sizes of as-prepared samples was annealed in vacuum at different temperatures. Figure 4 shows the XRD patterns of the sample S4 annealed under vacuum atmosphere (10^{-3} Pa) at 250, 350, 450, and 550 °C temperature individually. All observed peaks can be only indexed to the cubic phase of CoO, when the annealing temperature was equal to or lower than 350 °C. While the temperature was 450 °C

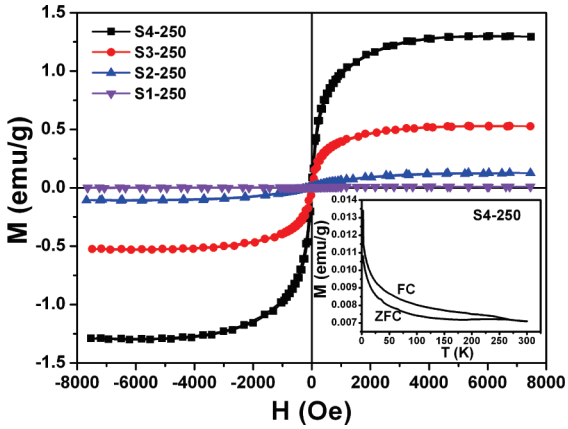

Figure 5. RT $M-H$ curves of different samples annealed under vacuum at 250 °C. The PM signals of the samples and the holder have been deducted. The inset shows the FC−ZFC curve of the sample S4-250.

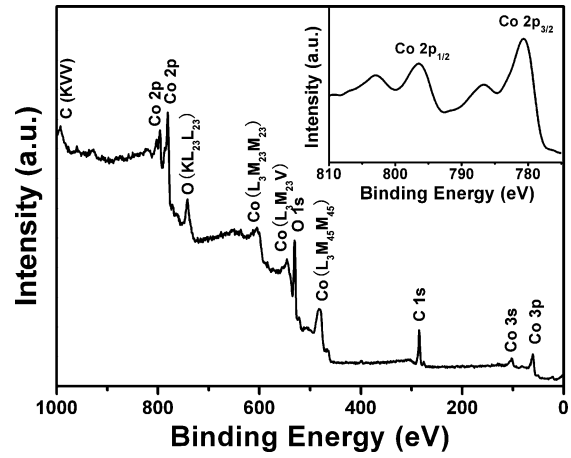

Figure 6. XPS survey spectrum for sample S4-250. The inset shows the high-resolution XPS spectrum of Co 2p at the energy range 770−810 eV.

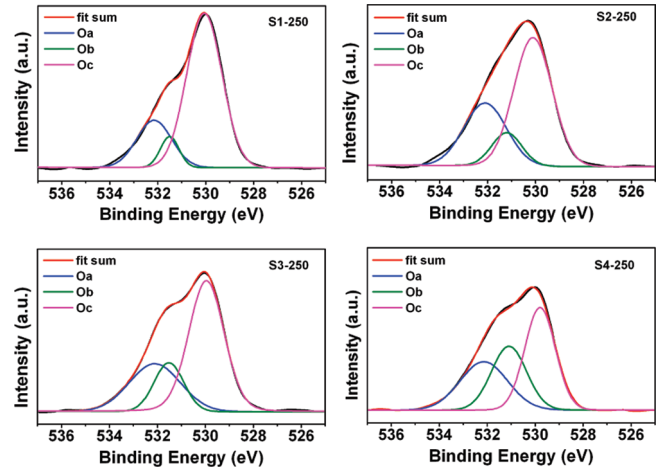

Figure 7. Fitted XPS spectra of O 1s for samples annealed under vacuum at 250 °C.

and higher, metal Co precipitated which became impurities in CoO nanospheres. The XRD pattern of the Co impurities can be indexed to be cubic phase (JCPDS card no. 89-4307). These results indicates that the optimum annealing temperature for all samples should be lower than 350 °C for preventing a precipitation of impure metal Co. In order to obtain pure CoO and induce enough oxygen vacancies, we choose the annealing temperature of 250 °C to study the FM of CoO nanospheres.

Figure 5 shows the magnetization versus magnetic field ($M-H$) curves of all CoO samples annealed in vacuum at 250 °C for 2 h. These samples were measured at RT with a maximum applied magnetic field of 8 kOe, and the paramagnetism (PM) signals of the samples and the holders were deducted. The hysteresis loops indicate that all CoO nanospheres under vacuum-annealing show FM at RT except for sample S1-250 which still shows PM. It is also seen that the magnetism of the samples is sensitive to CoO nanosphere diameters. The saturation magnetization (M_s) of CoO nanospheres decreases dramatically with the increase of nanosphere diameters, where the M_s for the sample S4-250 with the nanosphere sizes of about 40 nm shows the largest value (1.27 emu/g). The inset of Figure 5 shows zero-field-cooled (ZFC) and field-cooled (FC) magnetization curves in the temperature range of 2−330 K at the field of 100 Oe of sample S4-250 with the largest M_s. It can be seen that there is no blocking temperature in this temperature range. This indicates that there is no ferromagnetic cluster.

In order to further understand the physical origin of RT FM existing in these CoO nanospheres and clarify that all RT FM behavior comes from pure CoO nanospheres, the XPS technique was used to detect the chemical characteristics of all annealed samples. A representative XPS spectrum of sample S4-250 is shown in Figure 6. The result indicates that the sample was composed of Co and O elements. The inset of Figure 6 shows the XPS spectra of Co 2p core level. The peak at 780.2 eV can be assigned to Co $2p_{3/2}$ with the shakeup satellite at 786.1 eV, while the peak at 796.2 eV can be attributed to Co $2p_{1/2}$ with the satellite peak at 802.4 eV.[26] The presence of both peaks at 780.2 and 796.2 eV and their obvious satellite peaks indicates that the Co ions are in the +2 oxidation state.[27] The absence of the feature peak at 778.1 eV reveals that there is not any impurity of Co metal, consistent with the above XRD and SAED results.

As for the origin of the FM in the nonmagnetic oxides, several research groups have reported that the net magnetization observed in the materials, such as HfO_2, TiO_2, SnO_2, silicon, etc., might be attributed to the accidentally introduced ferromagnetic impurities.[28,29] Here, we believe that the observed magnetism in our vacuum-annealed CoO nanospheres cannot result from the magnetic impurities or artifact. This statement is based on the following: (1) No FM signal was observed from the as-prepared CoO and the capsules which were used to hold the samples during the magnetic measurements. This can rule out the contamination during the processes of experiments and measurements. (2) If there is metal Co in the samples with RT FM, the sample S1-250 may also show FM, because all samples are postannealed under the same conditions. Then, the Co impurities could be also ruled out. (3) Both ZFC−FC magnetization curves and XPS chemical analysis spectrum clearly reveal that the observed RT FM of vacuum-annealed CoO samples is intrinsic.

We deduce the RT FM of the vacuum-annealed CoO nanospheres origin from oxygen vacancies. Vacuum-annealing is proved to introduce some oxygen vacancies in oxides as others reported.[15,25,30,31] In order to verify this assumption, the O 1s XPS spectra of the CoO nanospheres were analyzed for comparison with others' reports.[32−34] Figure 7 depicts the multicomponent fitting to the O 1s peaks in samples S1-250, S2-250, S3-250, and S4-250, respectively. The broad and asymmetric nature of the peak is suggested to be due to the various coordinations of oxygen in CoO nanospheres. The O 1s XPS peak could be fitted into three peaks by Gaussian simulation.[35] The lowest binding energy peak located at 530.1

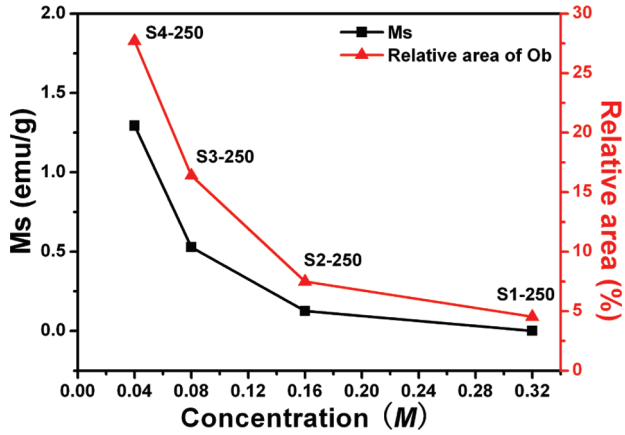

Figure 8. Solution concentration dependence of the M_s and relative area of the oxygen vacancies (Ob) for samples annealed under vacuum at 250 °C.

± 0.2 eV (Oa) can be assigned to O^{2-} ion in the CoO cubic structure, surrounded by the Co atoms with their full complement of the nearest-neighbor O^{2-} ions.[36] The highest binding energy peak at 532.4 ± 0.2 eV (Oc) is attributed to the near-surface oxygen, oxygen atoms in carbonate ions, surface hydroxylation, adsorbed H_2O, or O_2.[29] In addition, a new peak located at 531.2 ± 0.2 eV (Ob) appeared. Previous reports reveal that this peak could develop with the increasing loss of oxygen[37] and be associated with the O^{2-} ions in the oxygen-deficient regions (O vacancies) within the matrix of CoO.[32] Thus, the intensity of the medium binding energy component (Ob) may be related to the concentration of the oxygen vacancies. It can be seen that the concentration of the oxygen vacancy (Ob) increases with the decrease of CoO nanospheres diameter.

Figure 8 shows the M_s and the relative area of the oxygen vacancies as functions of the solution concentration. The sample S4-250 with the largest M_s exhibits the largest relative area of oxygen vacancies. The M_s and relative area of oxygen vacancies increase with the decrease of CoO nanosphere diameter, revealing that the relative intensities of the observed FM in CoO nanospheres under the vacuum-annealing could be related to the different surface-to-volume ratios. It is suggested that the oxygen atoms on the surface of CoO nanospheres can easily escape from the binding of the chemical bonds during the vacuum-annealing. The unpaired electrons then show the abnormal spin phenomenon causing the magnetism. The sample S4-250 has the smallest diameter, that is, the largest surface-to-volume ratio, which means the largest relative area of oxygen vacancies. Meanwhile, the M_s of S4-250 is the largest among the four samples. Conversely, S1-250 having the largest diameter and smallest surface-to-volume ratio remains a PM behavior. In a word, the oxygen vacancies on the surface of CoO nanospheres are suggested to be responsible for their RF FM behavior.

In addition, it is worth emphasizing that the SEM and XRD measurements (not given here) show that the annealing process under vacuum at 250 °C does not have any influence on the morphology and structure of the samples.

Conclusions

In summary, the single-crystalline and size-controlled pure CoO nanospheres were synthesized by the solvothermal method. RT FM of CoO nanospheres annealed in vacuum are investigated. The extrinsic impurity origin is excluded. A further simulation of the XPS data of O 1s spectra of all CoO nanospheres reveals that the origin of the FM should be attributed to the oxygen vacancies on the surface of individual CoO nanospheres. The intensity of FM of the samples is found to be proportional to the concentration of oxygen vacancies. Further theoretic investigations into the defects introducing FM are expected, and our work is on the way.

Acknowledgment. This work is supported by the National Science Fund for Distinguished Young Scholars (Grant No. 50925103), the Keygrant Project of Chinese Ministry of Education (Grant No. 309027), and the National Nature Science Foundation of China (Grant No. 11034004).

References and Notes

(1) Panigrahy, B. B.; Aslam, M.; Misra, D. S.; Ghosh, M.; Bahadur, D. *Adv. Funct. Mater.* **2010**, *20*, 1161.
(2) Li, M. J.; Ge, S. H.; Qiao, W.; Zhang, L.; Zuo, Y. L.; Yan, S. M. *Appl. Phys. Lett.* **2009**, *94*, 152511.
(3) Gao, D. Q.; Zhang, J.; Zhu, J. Y.; Qi, J.; Zhang, Z. H.; Sui, W. B.; Shi, H. G.; Xue, D. S. *Nanoscale Res. Lett.* **2010**, *5*, 769.
(4) Coey, J. M. D.; Venkatesan, M.; Stamenov, P.; Fitzgerald, C. B.; Dorneles, L. S. *Phys. Rev. B* **2005**, *72*, 024450.
(5) Zhang, L. Y.; Xue, D. S.; Gao, C. X. *J. Magn. Magn. Mater.* **2003**, *267*, 111.
(6) Araujo, C. M.; Kapilashrami, M.; Jun, X.; Jayakumar, O. D.; Nagar, S.; Wu, Y.; Arhammar, C.; Johansson, B.; Belova, L.; Ahuja, R.; Gehring, G. A.; Rao, K. V. *Appl. Phys. Lett.* **2010**, *96*, 232505.
(7) Dietl, T.; Ohno, H.; Matsukura, F.; Cibert, J.; Ferrand, D. *Science* **2000**, *287*, 1019.
(8) Coey, J. M. D.; Venkatesan, M.; Fitzgerald, C. B. *Nat. Mater.* **2005**, *4*, 173.
(9) Straumal, B. B.; Mazilkin, A. A.; Protasova, S. G.; Myatiev, A. A.; Straumal, P. B.; Schü tz, G.; van Aken, P. A.; Goering, E.; Baretzky, B. *Phys. Rev. B* **2009**, *79*, 205206.
(10) Potzger, K.; Zhou, S. Q.; Grenzer, J.; Helm, M.; Fassbender, J. *Appl. Phys. Lett.* **2008**, *92*, 182504.
(11) Pemmaraju, C. D.; Sanvito, S. *Phys. Rev. Lett.* **2005**, *94*, 217205.
(12) Shinde, S. R.; Ogale, S. B.; Higgins, J. S.; Zheng, H.; Millis, J. A.; Kulkarni, V. N.; Ramesh, R.; Greene, R. L.; Venkatesan, T. *Phys. Rev. Lett.* **2004**, *92*, 166601.
(13) Guillen, J. O.; Lany, S.; Barabash, S. V.; Zunger, A. *Phys. Rev. Lett.* **2006**, *96*, 107203.
(14) Gao, D. Q.; Zhang, Z. H.; Fu, J. L.; Xu, Y.; Qi, J.; Xue, D. S. *J. Appl. Phys.* **2009**, *105*, 113928.
(15) Sundaresan, A.; Bhargavi, R.; Rangarajan, N.; Siddesh, U.; Rao, C. N. R. *Phys. Rev. B* **2006**, *74*, 161306.
(16) Sundaresan, A.; Rao, C. N. R. *Nano Today* **2009**, *4*, 96.
(17) Risbud, A. S.; Snedeker, L. P.; Elcombe, M. M.; Cheetham, A. K.; Seshadri, R. *Chem. Mater.* **2005**, *17*, 834.
(18) Polshettiwar, V.; Baruwati, B.; Varma, R. S. *ACS Nano* **2009**, *3*, 728.
(19) Lin, H. K.; Chiu, H. C.; Tsai, H. C.; Chien, S. H.; Wang, C. B. *Catal. Lett.* **2003**, *88*, 169.
(20) Jiang, J.; Liu, J. P.; Ding, R. M.; Ji, X. X.; Hu, Y. Y.; Li, X.; Hu, A. Z.; Wu, F.; Zhu, Z. H.; Huang, X. T. *J. Phys. Chem. C* **2010**, *114*, 929.
(21) Jauch, W.; Reehuis, M.; Bleif, H. J.; Kubanek, F. *Phys. Rev. B* **2001**, *64*, 052102.
(22) Wdowik, U. D.; Parlinski, K. *Phys. Rev. B* **2008**, *77*, 115110.
(23) Dutta, D. P.; Sharma, G.; Manna, P. K.; Tyagi, A. K.; Yusuf, S. M. *Nanotechnology* **2008**, *19*, 245609.
(24) Kim, D.; Hong, J.; Park, Y. R.; Kim, K. J. *J. Phys.: Condens. Matter* **2009**, *21*, 195405.
(25) Ayyappan, S.; Raja, S. P.; Venkateswaran, C.; Philip, J.; Raj, B. *Appl. Phys. Lett.* **2010**, *96*, 143106.
(26) Yang, H. M.; Ouyang, J.; Tang, A. D. *J. Phys. Chem. B* **2007**, *111*, 8006.
(27) Ghosh, M.; Sampathkumaran, E. V.; Rao, C. N. R. *Chem. Mater.* **2005**, *17*, 2348.
(28) Abraham, D. W.; Frank, M. M.; Guha, S. *Appl. Phys. Lett.* **2005**, *87*, 252502.
(29) Grace, B. P. J.; Venkatesan, M.; Alaria, J.; Coey, J. M. D.; Kopnov, G.; Naaman, R. *Adv. Mater.* **2009**, *21*, 71.
(30) Hong, N. H.; Sakai, J.; Poirot, N.; Brize, V. *Phys. Rev. B* **2006**, *73*, 132404.

(31) Venkatesan, M.; Fitzgerald, C. B.; Coey, J. M. D. *Nature* **2004**, *430*, 630.
(32) Gao, D. Q.; Zhang, J.; Yang, G. J.; Zhang, J. L.; Shi, Z. H.; Qi, J.; Zhang, Z. H.; Xue, D. S. *J. Phys. Chem. C* **2010**, *114*, 13477.
(33) Pendey, B.; Ghosh, S.; Srivastava, P.; Kumar, P.; Kanjilal, D. *J. Appl. Phys.* **2009**, *105*, 033909.
(34) Fan, J. C. C.; Goodenough, J. B. *J. Appl. Phys.* **1977**, *48*, 3524.
(35) Chen, M.; Wang, X.; Yu, Y. H.; Pei, Z. L.; Bai, X. D.; Sun, C.; Huang, R. F.; Wen, L. S. *Appl. Surf. Sci.* **2000**, *158*, 134.
(36) Natile, M. M.; Glisenti, A. *Chem. Mater.* **2002**, *14*, 3090.
(37) Naeem, M.; Hasanain, S. K.; Kobayashi, M.; Ishida, Y.; Fujimori, A.; Buzby, S.; Shah, S. I. *Nanotechnology* **2006**, *17*, 2675.

JP106818P